J. Pineal Res. 2004; 37:55–70
Doi:10.1111/j.1600-079X.2004.00140.x

Journal of Pineal Research

Visualization of the antioxidative effects of melatonin at the mitochondrial level during oxidative stress-induced apoptosis of rat brain astrocytes

Mei-Jie Jou[1], Tsung-I Peng[2], Russel J. Reiter[3], Shuo-Bin Jou[4], Hong-Yueh Wu[1] and Shiau-Ting Wen[1]

[1]Department of Physiology and Pharmacology, Chang Gung University, Tao-Yuan; [2]Department of Neurology, Lin-Kou Medical Center, Chang Gung Memorial Hospital, Tao-Yuan, Taiwan; [3]Department of Cellular and Structural Biology, The University of Texas Health Science Center at San Antonio, San Antonio, Texas, USA; [4]Department of Neurology, China Medical University, Taichung, Taiwan

Abstract: Oxidative stress-induced mitochondrial dysfunction has been shown to play a crucial role in the pathogenesis of a wide range of diseases. Protecting mitochondrial function, therefore, is vital for cells to survive during these disease processes. In this study, we demonstrate that melatonin, a chief secretory product of the pineal gland, readily rescued mitochondria from oxidative stress-induced dysfunction and effectively prevented subsequent apoptotic events and death in rat brain astrocytes (RBA-1). The early protection provided by melatonin in mitochondria of intact living cells was investigated by the application of time-lapse conventional, confocal, and multiphoton fluorescent imaging microscopy coupled with noninvasive mitochondria-targeted fluorescent probes. In particular, we observed that melatonin effectively prevented exogenously applied H_2O_2-induced mitochondrial swelling in rat brain astrocytes at an early time point (within 10 min) and subsequently reduced apoptotic cell death (150 min later). Other early apoptotic events such as plasma membrane exposure of phosphatidyl serine and the positive YOPRO-1 staining of the early apoptotic nucleus were also prevented by melatonin. A mechanistic study at the mitochondrial level related to the early protection provided by melatonin revealed that the indole molecule significantly reduced mitochondrial reactive oxygen species (ROS) formation induced by H_2O_2 stress. Melatonin also prevented mitochondrial ROS generation caused by other organic hydroperoxides including *tert*-butyl hydroperoxide and cumene hydroperoxide. This antioxidative effect of melatonin is more potent than that of vitamin E. Via its ability to reduce mitochondrial ROS generation, melatonin prevented H_2O_2-induced mitochondrial calcium overload, mitochondrial membrane potential depolarization, and the opening of the mitochondrial permeability transition (MPT) pore. As a result, melatonin blocked MPT-dependent cytochrome c release, the downstream activation of caspase 3, the condensation and karyorrhexis of the nucleus and apoptotic fragmentation of nuclear DNA. Thus, the powerful mitochondrial protection provided by melatonin reinforces its therapeutic potential to combat a variety of oxidative stress-induced mitochondrial dysfunctions as well as mitochondria-mediated apoptosis in various diseases.

Key words: antioxidant, apoptosis, melatonin, mitochondria, mitochondrial reactive oxygen species

Address reprint requests to Mei-Jie Jou, Department of Pharmacology, Chang Gung University, 259 Wen-Hwa 1st Road, Kwei-Shan, Tao-Yuan 333, Taiwan.
E-mail: mjjou@mail.cgu.edu.tw

Received December 15, 2003;
accepted March 16, 2004.

Introduction

Oxidative insults resulting from either an excessive generation of reactive oxygen species (ROS) or the deterioration of antioxidant defense capacity has been closely linked to the pathogenesis of neuronal degeneration [1–4]. Maintenance of an appropriate activity of the endogenous antioxidative defense system, therefore, plays a pivotal role in clinical prevention and treatment of ROS-associated neuronal degeneration and diseases. Melatonin, the chief secretory product of the pineal gland, has frequently been documented to be a potent cellular antioxidant and can effectively scavenge toxic free radicals and associated reactants [5, 6]. For example, melatonin dzirectly scavenges singlet oxygen ($^1O_2$), hydrogen peroxide (H_2O_2) and the devastatingly toxic hydroxyl radical ($^{\bullet}OH$) [7–11]. In addition, melatonin stimulates mRNA levels and activities of antioxidative enzymes including superoxide dismutase (SOD), glutathione peroxidase (GPx), and glutathione reductase (GRx) [5, 12]. Thereby, these multiple actions of melatonin protect cells from ROS-mediated lipid peroxidation, protein destruction and nuclear DNA damage [13–20].

Recently, additional evidence suggests that melatonin may directly act at the mitochondrial level to reduce

mitochondrial oxidative stress-induced damage [21, 22]. For example, the toxicity of cyanide, a drug which blocks complex IV of the mitochondrial electron transport chain (ETC), is reversed by melatonin [23]. The actions of neurotoxins including 6-hydroxydopamine, kainic acid [24, 25] and 1-methyl-4-phenylpyridinium [26] induced dysfunction of complex I of the mitochondrial respiratory chain are prevented by melatonin. Moreover, melatonin increases the activities of the respiratory chain complexes I and IV and prevents mitochondrial damage induced by an inorganic polycationic complex, ruthenium red, which inhibits the mitochondrial Ca^{2+} uniporter for Ca^{2+} uptake and acts to cause mitochondrial uncoupling and oxidative stress [17]. Furthermore, melatonin stimulated the activities of the oxidative phosphorylation enzymes and the production of ATP [27]. Acutely administered melatonin restores hepatic mitochondrial physiology in aging mice, particularly complex I and IV activities, and limits ischemia- and reperfusion-induced mitochondrial injury [28, 29].

In addition, our recent studies demonstrate that melatonin significantly reduced laser irradiation-induced mitochondrial ROS formation and apoptosis in RBA-1 cells [30]. Melatonin also protects against mitochondrial DNA mutation and deletion caused oxidative damage and apoptosis [31]. Given that mitochondria are a major cellular ROS source and, unavoidably, are frequent targets of ROS damage as well as crucial role of mitochondria in executing cell apoptosis [2, 32–34], the precise cellular mechanisms of action of melatonin at the mitochondrial level, thus, require investigation.

In an attempt to visualize how the indole rescues mitochondria from oxidative stress-induced dysfunction and, as a consequence, effectively prevents subsequent apoptotic events and cell death, the present study employed a conventional imaging technique together with advanced confocal and multi-photon laser scanning fluorescence microscopy coupled with noninvasive mitochondria-targeted fluorescent probes. Specifically, time-lapse imaging of the dynamic profiles of mitochondrial function which were protected by melatonin during exogenously applied H_2O_2-induced apoptosis were studied. The end points included mitochondrial morphology, mitochondrial membrane potential, mitochondrial ROS formation, and mitochondrial calcium regulation, as well as subsequent apoptotic events including opening of the mitochondrial permeability transition (MPT) pore, release of cytochrome c, caspase-3 activation, nuclear condensation and DNA fragmentation. Early ROS-associated events including the exposure of phosphatidyl serine (PS) and early apoptotic nuclei were also investigated. Rat brain astrocytes (RBA-1) were used for these studies because of their potential role in neuronal survival during high oxidative stress conditions.

Materials and methods

Cell preparation

Normal rat brain astrocytes (RBA-1) used for this study were originally established through a continuous passage of primary astrocytes isolated from 3-day-old JAR-2, F51 rat brains by Dr Teh-Cheng Jou [35]. All cells were grown in Dulbecco's modified Eagle's medium (Life Technologies, Grand Island, NY, USA) supplemented with 10% (v/v) fetal bovine serum. The cells were plated onto glass coverslips (Model No. 1, VWR Scientific, San Francisco, CA, USA) coated with poly-L-lysin. Experiments were preformed after cells grew to 80–90% (about 2–3 culture days) of confluence.

Chemicals and fluorescent dyes loading for studying mitochondrial function

All chemicals were obtained from Sigma (St Louis, MO, USA) and fluorescent dyes were purchased from Molecular Probes Inc. (Eugene, OR, USA). Mitochondrial function was studied by imaging mitochondrial morphology, mitochondrial ROS formation, mitochondrial membrane potential changes, mitochondrial calcium regulation and the opening of the MPT using specific fluorescent probes. To image mitochondrial morphology, cells were loaded with a mitochondrial-targeted fluorescent probe, MitoTracker Green (Mito-G, giving a green fluorescence) or MitoTracker Red (Mito-R, giving a red fluorescence), both at concentration of 100 nM. Mitochondrial membrane potential was detected using either 200 nM JC-1 or 300 nM tetramethyl rhodamine ethyl ester (TMRM). Intracellular ROS formation and mitochondrial ROS were visualized using the acetyl ester form of 2 μM dichlorofuorescin (DCF-DA) and 100 nM dihydrorhodamine 123 (D-123), respectively. Mitochondrial calcium was detected using 1 μM Rhod-2/AM. Nucleic acid was stained with 1 μM propidium iodide (PI) to identify dead cells. Fluorescent probes were all loaded at room temperature for 20–30 min. After loading, cells were rinsed three times with HEPES-buffered saline (in mM: 140 NaCl, 5 KCl, 1 $MgCl_2$, 2 $CaCl_2$, 10 glucose, 5 HEPES, pH 7.4). For all ester forms of dyes including DCF-DA and Rhod-2/AM, cells were treated for an extra 40 min after dye loading to allow cleavage of the ester form of dye to its acid form.

Fluorescence conventional and multiphoton imaging microscopy

All phase-contrast and conventional fluorescence images were obtained using a Zeiss inverted microscope (AxioVert 200M, Carl Zeiss, Jena, Germany) equipped with a mercury lamp (HBO 103), a cool CCD camera (Coolsnap fx, Roper Scientific, Tucson, AZ, USA), and Zeiss objectives (Plan-NeoFluar 100×, N.A. 1.3 oil). Filters used for detecting DCF and Mito-G was No. 10 (Exi: BP 450–490 nm; Emi: BP 515–565 nm) and for Mito-R and TMRM the filter was No. 15 (Exi: BP 546/12 nm; Emi: LP 590 nm). Confocal images of cells and mitochondria were collected on a Bio-Rad Radiance 2100 using 488 nm Argon laser illumination (Bio-Rad, Hercules, CA, USA). To avoid single photon-induced autolysis of DCF/DA, multiphoton illumination was applied as previous described [36]. Multiphoton fluorescence images were collected on a Leica SP2 MP (Leica-Microsystems, Mannheim, Germany) fiber coupling system equipped with a Ti:Sa-Laser system (model: Millenia/Tsunami; Spectra-Physics) providing a pulse repetition rate at 82 MHz, laser pulse width of 1.2 picoseconds, a spectral

bandwidth of 1 nm and object pulse width of 1.3 picoseconds). Wavelength at 800 nm with an average laser power of 600 mW was selected for illumination. During fluorescence imaging, the illumination light was reduced to the minimal level by using appropriate neutral density filters to prevent the photosensitizing effects due to the interaction of light with fluorescent probes including bleaching and auto-oxidation of the fluorescent probes. All images were processed and analyzed using MetaMorph software (Universal Imaging Corp., West Chester, PA, USA). Intensity levels were analyzed from the original images and graphed using Microsoft EXCEL software and Photoshop. Pseudo-color display with a scale ranged from 0 to 255 units was used to enhance the contrast of the fluorescence changes for each image.

Imaging oxidant-induced ROS formation

In this study, oxidative stress was introduced by exogenously exposing RBA-1 cells to various oxidants for 10 min. The concentrations of oxidants used in this study were selected with an intention to induced rapid apoptosis (within 3 hr) in order to make feasible long-term continuous confocal fluorescence imaging recordings. In many cases, cells were exposed to oxidative stress by treating them with 10 mM H_2O_2 for 10 min. Intracellular ROS were detected using an intracellular ROS dye, DCF-DA, as previous described [30, 37]. DCF-DA is a membrane-permeable form of dye that diffuses across lipid membranes. The nonfluorescent DCF-DA is oxidized by intracellular ROS to form the highly fluorescent DCF. In DCF images, mitochondrial ROS was calculated from areas based on fluorescent image of Mito-R or phase-contrast image of mitochondrial distribution from the same cell. Mitochondrial ROS were also detected using D123. After loading, the nonfluorescent D123 is converted to the fluorescent product, rhodamine 123, by an interaction with reactive oxygen intermediates. Both DCF and D123 images were taken to confirm mitochondrial ROS formation using the time-lapse mode of LSCM. Multiphoton illumination has particular benefits for long-term recording of ROS formation using DCF and D123 as these probes readily undergo light-sensitive auto-oxidation during single-photon illumination [30, 36]. Images of ROS were obtained and displayed with a pseudo-color scale from 0 to 255 units. Intensity values were analyzed per pixel from the cytosolic, the mitochondrial and the nuclear area of the cells. Fluorescence intensity changes in the experiments with DCF were normalized with the control. Differences were evaluated using the Student's *t*-test.

Fluorescence measurement of intracellular ROS or mitochondrial ROS with FACS

Intracellular ROS generation was measured in a group of cells using ROS probes with fluorescence detected by flow cytometry (FACS, Becton-Dickson FACScan, San Jose, CA, USA). In brief, RBA-1 cells were grown to 70% confluent density and were then incubated in the dark with either DCF-DA or D-123 as described for fluorescence microscopy, scraped, and resuspended in HEPES buffer solution. The mean of DCF and D-123 fluorescence intensity were obtained from 10,000 cells using 480 nm excitation and 540 nm emission settings. ROS formation was stimulated by treatment of cells with different doses of oxidants including H_2O_2, *tert*-butyl hydroperoxide (*t*Bu-OOH) and cumene hydroperoxide (Cu-OOH) for 10 min. Cells were then rinsed with HEPES solution and loaded onto the FACS for ROS measurement at different time points after oxidant treatment. FL-1 fluorescence was recorded, and cellular debris was electronically gated out based on the forward light scatter. By use of the same settings, the fluorescence was quantified for each experimental group. Fluorescence data are expressed as net fluorescence increase or as percent increase over untreated samples.

Apoptotic cell analysis

Early apoptotic nuclei (before condensation and fragmentation) was detected using a Vybrant Apoptosis Assay Kit #4 (Molecular Probes) which contains the green fluorescent YO-PRO-1 and the red fluorescent PI. During early stages of apoptosis, the cytoplasmic membrane becomes lightly permeated with the green fluorescent YO-PRO-1 dye, while PI does not enter the membranes until late apoptotic stages. Thus, positive staining with YO-PRO-1 provides an early detection of an apoptotic nucleus [38]. Briefly, cells were incubated with 1 μL YOPRO-1 stock solution (Component A) and 1 μL PI stock solution (Component B) from a Vybrant Apoptosis Assay Kit #4 for 20–30 min prior to oxidative stress exposure. Time-lapse confocal fluorescent images of YO-PRO-1, and PI were taken continuously and immediately after apoptosis induction using H_2O_2 to precisely detect the time point of positive early YO-PRO-1 nuclear staining. Late apoptotic characteristics of condensation and fragmentation of the nucleus were identified by both phase-contrast and fluorescent PI image. Nuclear sizes of cells prior to and after H_2O_2 treatment were analyzed using MetaMorph software.

Detecting phosphatidylserine (PS) externalization during apoptosis was determined as follows. The flip-flop of PS from the inner- to the outer-plasma-membrane leaflet during apoptosis is a common phenomenon in apoptosis and it occurs in most cell types independent of apoptotic inducers. Exposure of PS is an early event that precedes cell shrinkage and nuclear condensation [39, 40]. PS exposure induced by H_2O_2 stress in RBA-1 cells was detected by FITC-conjugated Annexin V-FITC staining; this is seen as green fluorescence on the plasma membrane during the occurrence of PS externalization. The precise time point for PS exposure and its relation to mitochondrial ROS formation were carefully determined by time-lapse imaging of cells dual labeled with Annexin V-FITC and D-213 after they were exposed to H_2O_2, using laser scanning imaging microscopy.

Release of cytochrome c in fixed cells was detected by immunocytochemistry (ICC). Briefly, cultured cells were fixed with 3.7% paraformaldehyde in culture medium for 15 min. Cells were then washed with PBS twice and were permeabilized with 0.5% Triton X-100 for 10 min. Cells were then washed twice with PBS and incubated with 1%

BSA for 30 min and then tagged with first monoclonal antibody of cytochrome c (BioVision Research Products, Mountain View, CA, USA) and second goat anti-mouse polyclonal Ab conjugated with FITC (Jackson Immuno Research Lab, Inc., West Grove, PA, USA). Cells were visualized using a confocal microscope with 100× oil immersion objective.

Caspase-3 activity was measured by using a Caspase-3 Colorimetric Assay Kit as the manufacturer described (BioVision, Inc.). Briefly, cells, after being treated with H_2O_2 with or without melatonin co-incubation, were washed once with PBS and collected. Cytosolic extracts obtained using Cell Lysis Buffer were then incubated with DEVD-pNA substrate for 1–2 hr and read at 400-nm in a microtiter plate reader. Background reading from cell lysates and buffers were subtracted from the readings from all samples before calculating the fold-increase in caspase-3 activity.

Apoptotic DNA ladders were analyzed using the Apo-Alert LM-PCR^{TM} Ladder Assay Kit from Clontech (Palo Alto, CA, USA) which specially amplified nucleosomal ladders generated during apoptosis. Briefly, cellular DNA was collected from control cells and cells treated with H_2O_2 with or without the presence of melatonin. The extracts were treated with RNase A and Proteinase K. The LM-PCR assay was performed according to the user manual (15 PCR cycles). A quantity of 15 μL of each PCR products was electrophoresed on a 1.2% agarose/EtBr gel at 6 V/cm for approximately 2.5 hr and DNA was detected by ethidium bromide under UV light.

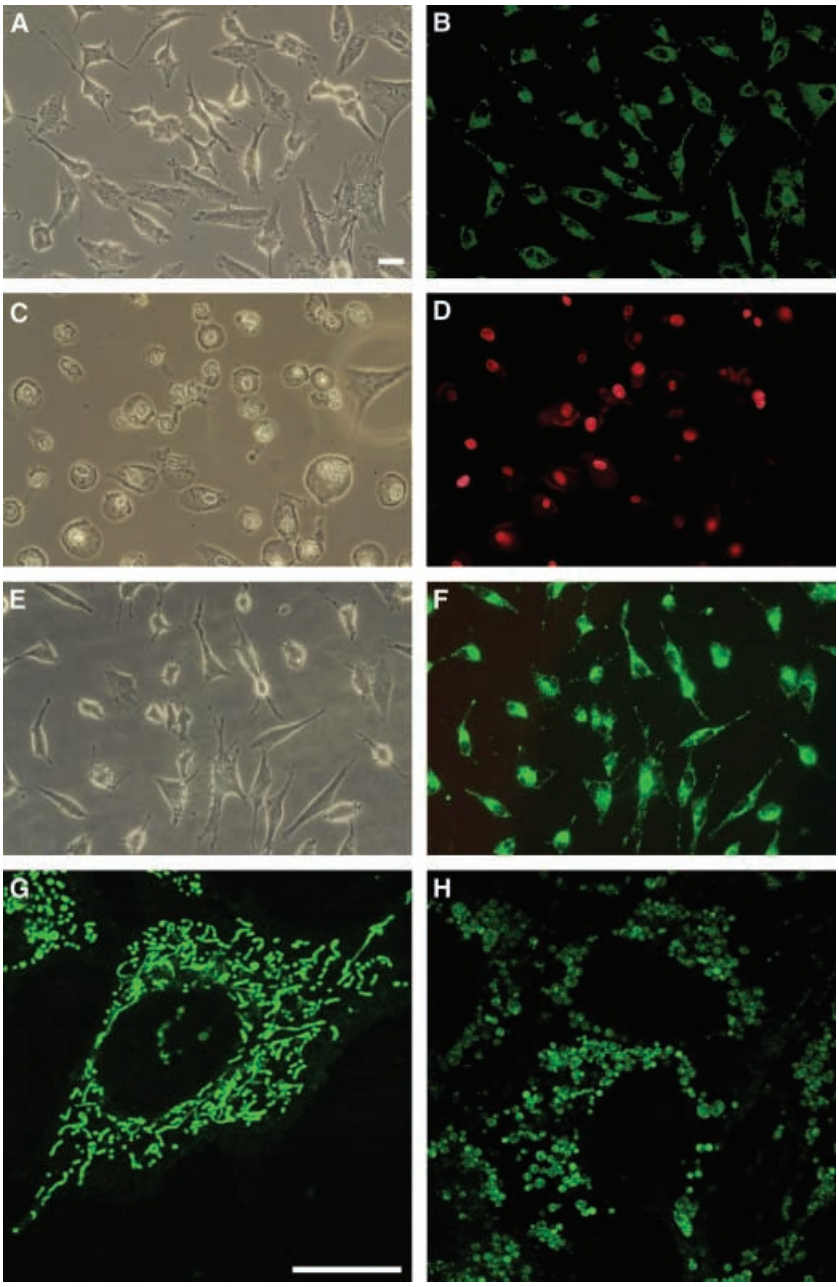

Fig. 1. Melatonin prevented H_2O_2-induced plasma membrane blebbing, mitochondrial swelling, nuclear condensation and apoptotic cell death in RBA-1 cells. (A, B) Control; (C, D) 200 min after exposure to H_2O_2; (E, F) melatonin protected cells at 300 min after exposure to H_2O_2; (G, H) 100× confocal fluorescent images of mitochondria of a live RBA-1 cell. (A, C, E) 40× phase-contrast images. (B, D, F) 40× conventional dual fluorescent staining of Mito-G and PI for evaluating mitochondrial morphology and nuclei of dead cells, respectively. (A–D) Images taken from the same cells. Note that 200 min after exposure to H_2O_2, cells formed apoptotic blebs on the plasma membranes, lost Mito-G staining completely, and showed positive PI nuclear staining in the condensed nuclei. In contrast to C and D, RBA-1 cells protected with 100 μM melatonin significantly maintained plasma membrane integrity and positive Mito-G and negative PI staining even at 300 min after exposure to H_2O_2. (G) Melatonin protected mitochondria after exposure to H_2O_2. (H) Mitochondria without melatonin protection after exposure to H_2O_2. Bar, 10 μM.

Results

The potent cytoprotective effect provided by melatonin was observed in RBA-1 astrocytes that were exposed to 10 mM H_2O_2 for 10 min to induce apoptotic cell death. Cellular as well as mitochondrial morphological alteration induced by the H_2O_2 stress were imaged by both conventional phase-contrast and confocal fluorescence imaging microscopy coupled with a noninvasive mitochondria-targeted fluorescent marker, Mito-G or Mito-R. As shown in Fig. 1, the control astrocytes maintained well-differentiated astrocytic processes (Fig. 1A) and readily retained the Mito-G staining (Fig. 1B). In contrast to the control cells, 200 min after the H_2O_2 exposure, cells formed marked plasma membrane blebs (Fig. 1C), lost the ability to retain Mito-G, and showed positive nuclear PI staining as an indication of cell death (Fig. 1D). Also note that the size of nuclei of the H_2O_2-treated cells was condensed to $<50\%$ of that of the control cells indicating a typical apoptotic death. The potent cytoprotective effect provided by melatonin is shown in Fig. 1E,F where 100 μM melatonin is seen to significantly reverse the cytotoxic effect of H_2O_2. In the melatonin-protected cells, cellular morphology as well as the fluorescence of Mito-G were well preserved long after the H_2O_2 exposure. In addition, nuclear PI staining was not observed in cells incubated with melatonin even at 300 min after the H_2O_2 stress. The marked protection of mitochondrial morphology provided by melatonin after the H_2O_2 treatment was further visualized by laser scanning confocal imaging microscopy. As shown in Fig. 1G, with the protection provided by melatonin the mitochondria retained their typical rod- or thread-like morphology even after 300 min of H_2O_2 exposure. Conversely, without melatonin protection mitochondria swelled and assumed a circular shape after H_2O_2 stress (Fig. 1H).

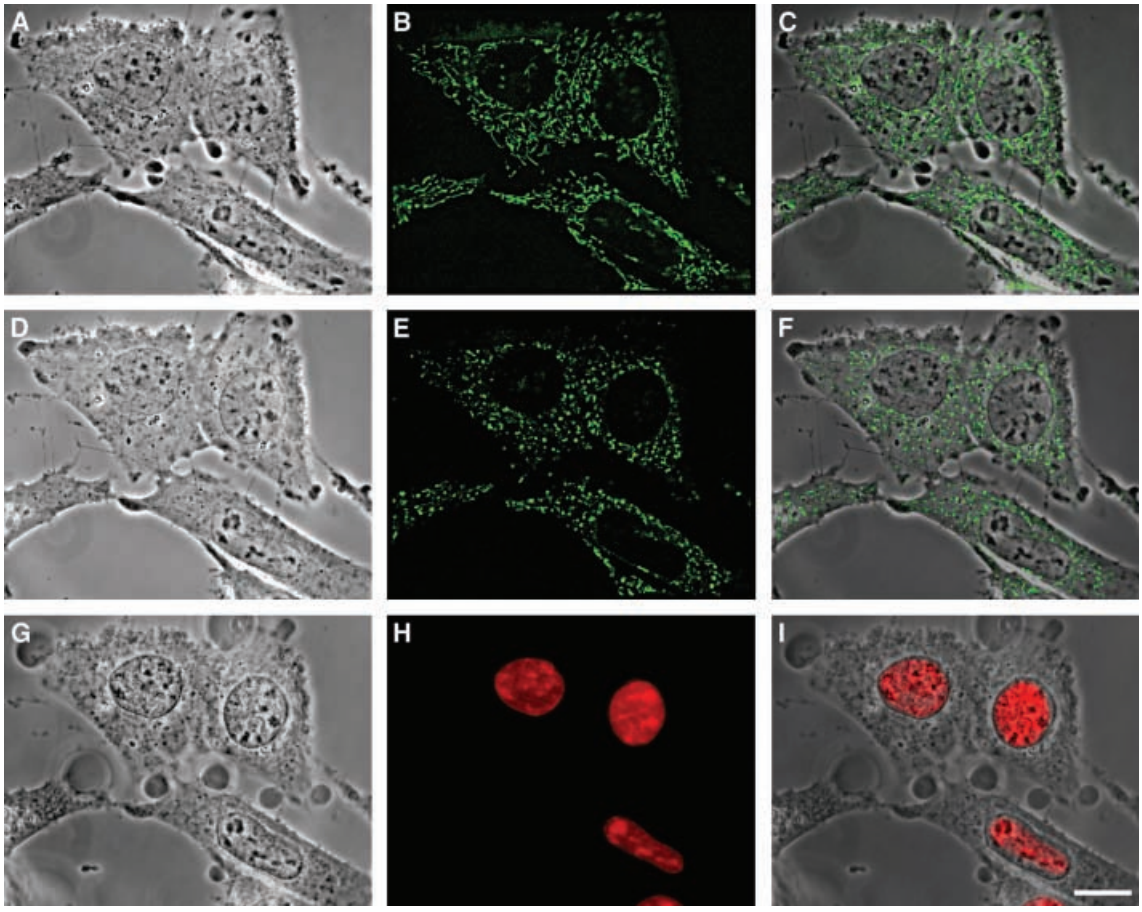

Fig. 2. The precise time point for the appearance of the MPT, plasma membrane blebbing and nuclear PI staining induced by H_2O_2 stress. MPT opening was detected by continuously recording cell and mitochondrial morphology every 2 min for 30 min and then every 10 min for 2.5 hr after H_2O_2 exposure. The active process is documented in a time-lapse movie file, mitomovie.avi, (Please refer to Supplementary Material section for information on how to access this). Representative images at selected time points show that mitochondrial damage appeared at a relative early time point during oxidative stress-induced apoptosis. (A, D, G) Phase-contrast images; (B, E, H) dual fluorescence images of Mito-G and PI; (C, F, I) superimposed images of phase-contrast and dual labeling fluorescence images of the same cells. The precise time point for the occurrence of MPT opening was at 10 min after H_2O_2 exposure (E). Note that the morphology of cells and nuclei, however, appeared similar to that of the control cells at this time point during H_2O_2 stress. Severe plasma membrane blebbing occurred 50 min after the initiation of oxidative stress (G). Cells completely lost Mito-G staining of mitochondria at 60 min after oxidative stress (not shown). Positive PI staining of the nuclei, however, did not appear until 130 min after oxidative stress (H). Note the plasma membrane blebbing and nuclear condensation at this time point. Bar, 10 μM.

The swollen mitochondria is an indication of the opening of a mitochondrial mega channel, the MPT pore, which has been reported to be closely associated with the subsequent release of mitochondrial lethal proteins and downstream activation of apoptotic events. To determine the precise time point of MPT opening and its relation to cellular morphology and plasma membrane integrity after H_2O_2 exposure, we used time-lapse measurements and recorded the detailed changes in cellular as well as mitochondrial morphology during the entire apoptotic cell death process induced by H_2O_2. As shown in Fig. 2, phase-contrast images of control cells demonstrated phase-dense (gray color) mitochondria which were evenly distributed in the cytoplasm (Fig. 2A). Mito-G staining revealed typical rod- or thread-shaped healthy mitochondria (Fig. 2B) which co-localized well with the gray phase-dense mitochondria (Fig. 2C). The effect of oxidative stress on mitochondrial morphology was rapid and occurred immediately after H_2O_2 exposure. Mitochondria began to swell quickly on exposure to H_2O_2. Ten minutes after the H_2O_2 stress, mitochondria were markedly swollen (Fig. 2E). The morphology of cells after H_2O_2 stress, however, appeared similar to that of the control cells except that the phase dense gray mitochondria in the cytosolic area became much lighter due to the swelling of mitochondria (Fig. 2D). Severe plasma membrane blebbing (Fig. 2G) and cell death identified by positive PI staining of the nuclei (Fig. 2H), however, did not appear until 200 min after the H_2O_2 treatment. Mitochondria at this stage completely lost their ability to retain Mito-G and nuclei were slightly condensed (Fig. 2H). Superimposed images of phase-contrast and fluorescent images of Mito-G and PI taken at each time

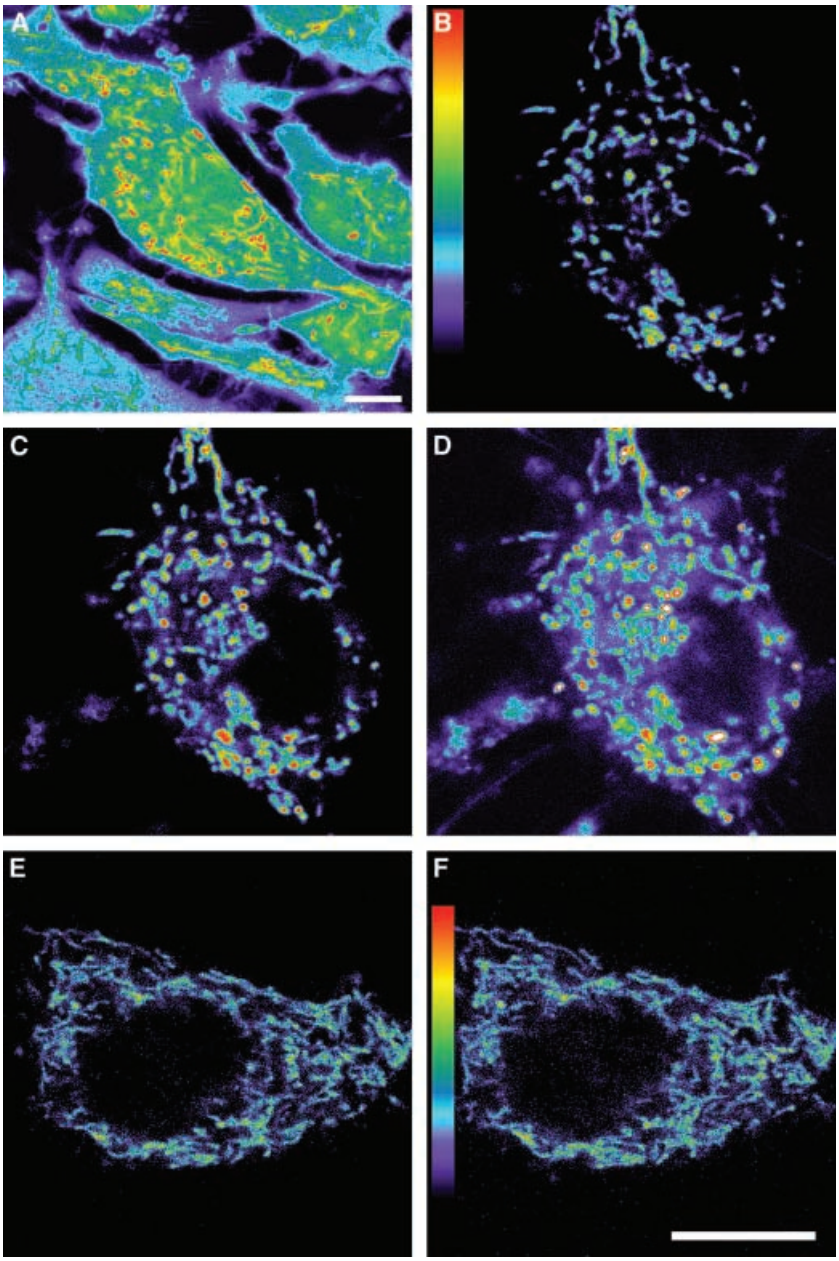

Fig. 3. Intracellular ROS distribution and significant prevention of mitochondrial ROS formation by melatonin after oxidant exposure. (A) An enhanced pseudo-color image demonstrating mitochondrial ROS levels were much higher than ROS levels in other compartments. Note the rod- or thread-like mitochondria in yellow to red pseudo-color, whereas the nuclear and cytosolic areas were in purple to blue pseudo-color. (B–D) Mitochondrial ROS formation measured by time-lapse photography using D-123 after H_2O_2 stress: (B) control; (C) 5 min; (D) 10 min after H_2O_2 exposure. Note the pseudo-color of D-123 in the mitochondria of an astrocyte increased rapidly after the H_2O_2 stress and was later accompanied by the MPT (mitochondrial swelling). (E and F) Melatonin significantly prevented mitochondrial ROS formation as well as the MPT opening induced by H_2O_2 stress. Bar, 10 μM.

point demonstrate that mitochondrial disruption was a relatively early event (within 10–20 min) as compared with plasma membrane blebbing and positive PI staining of the nuclei (200 min after the stress) during H_2O_2-induced apoptosis (Fig. 2I). To further demonstrate that the early protection of mitochondria is critical for preventing subsequent oxidative stress-induced cell death, we applied melatonin at different time points during the death process induced by H_2O_2. Intriguingly, melatonin, when administrated after H_2O_2 stress, particularly at the time points after the occurrence of the MPT opening, completely lost its ability to rescue the mitochondria including the ability for mitochondria to retain Mito-G, reverse the opening of MPT and plasma membrane blebbing, and to prevent PI nuclear staining (results not shown). These observations strongly indicate that mitochondria are the 'point of no return' and early protection of mitochondrial function provided by melatonin is particularly pivotal in the prevention of the entire apoptotic death processes induced by H_2O_2.

To determine whether the early mitochondrial protection provided by melatonin is due to its anti-mitochondrial ROS formation during the first 10–20 min after the H_2O_2 stress, we measured cellular and mitochondrial ROS levels using confocal imaging microscopy coupled with ROS probes after oxidant exposure. ROS probes including DCF and D123 were used to record intracellular ROS formation. In addition, multi-photon imaging microcopy was supplemented for ROS measurement as the longer wavelengths of multiphoton illumination significantly reduced the photo-irradiation induced photo-bleaching and auto-oxidation of ROS probes and benefited particularly the long-term mitochondrial ROS recording from intact living cells [36]. Similar to our previous observations, a DCF pseudo-color image clearly demonstrated that intracellular ROS levels of resting cells are rather heterogeneous. The ROS levels in cytosol, nucleus and mitochondria were roughly at a ratio of 0.29:0.33:1, respectively ($n = 8$, Fig. 3A). The 2–3 times higher mitochondrial ROS levels compared with that from other compartments further confirms that mitochondria indeed are a major source for intracellular ROS. We then measured mitochondrial ROS formation after H_2O_2 stress using D123. As shown in Fig. 3B–D, the time-lapse fluorescent signal of D123 of single astrocytes demonstrated that mROS increased rapidly (within 10 min) after cells were exposed to H_2O_2 and this was later accompanied by mitochondrial swelling and cell shrinkage. Note that in some areas of the mitochondria, mitochondrial ROS increase preceded mitochondrial swelling indicating that opening of the MPT appeared after mitochondrial ROS formation. Melatonin significantly reduced mitochondrial ROS formation as well as the MPT opening induced by the H_2O_2 stress (Fig. 3E,F). We repeatedly observed that melatonin slightly reduced basal level of ROS as shown in Fig. 3E. Continuous changes in mitochondrial ROS detected by time-lapse D-123 imaging during the first 10 min after H_2O_2 exposure was analyzed in Fig. 4. The potent anti-mitochondrial ROS formation provided by melatonin during the early stage of H_2O_2 exposure is well demonstrated.

The effect of anti-ROS formation provided by melatonin was further detected using FACS coupled with the ROS

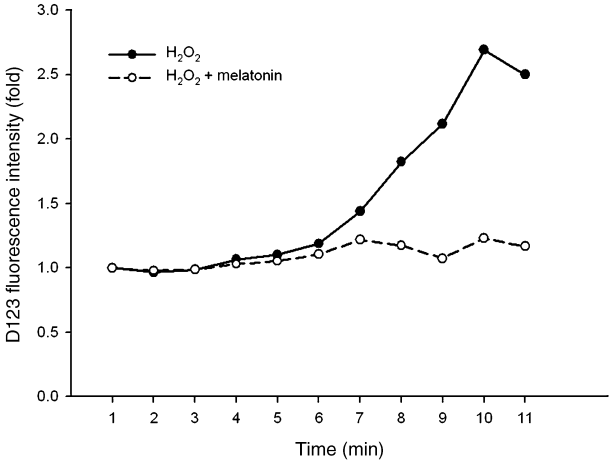

Fig. 4. Fluorescence intensity analyzed from D-123 confocal images during the first 11 minutes after the H_2O_2 stress in the absence and presence of melatonin. Note the potent anti-ROS generation effect provided by melatonin of H_2O_2 stress-induced apoptosis.

probes, DCF (Fig. 5A–E) or D-123 (Figs 5F and 6), where ROS formation from a group of cells was measured. We compared the anti-ROS formation effect provided by melatonin with that of other antioxidants. Effects of melatonin on short-chain oxidants including *t*Bu-OOH and Cu-OOH-induced oxidative stress were also compared. Fig. 5A demonstrates a dose-dependent elevation of ROS formation induced by increasing concentrations of H_2O_2 (0.1, 1 and 10 mM). Cells pretreated with 1–500 μM melatonin dose-dependently reduced the H_2O_2 stress-induced ROS formation. As shown in Fig. 5B, 100 μM melatonin significantly reduced the H_2O_2-(0.1, 1 and 10 mM) induced ROS formation. In addition, note that melatonin slightly decreased the resting ROS levels. The antioxidative activity of melatonin was found to be more potent than that of 100 or 500 μM vitamin E (Figs 5C and 6). A higher concentration of melatonin (500 μM), however, provided a similar effect as that of a lower concentration (100 μM) (Fig. 6). The anti-ROS formation action of melatonin was not limited to H_2O_2, as melatonin also reduced ROS formation induced by *t*Bu-OOH and Cu-OOH (Fig. 5D,E) respectively. The anti-mitochondrial ROS formation effect of melatonin detected by D-123 showed similar results (Figs 5F and 6).

As mitochondrial calcium dysregulation is often recognized as an early sign of mitochondrial dysfunction and as it trigger MPT opening during oxidative stress, we measured dynamic changes in mitochondrial Ca^{2+} concentrations and mitochondrial morphology simultaneously. In the control cells, mitochondria maintained their rod or thread shape (Fig. 7A) and calcium concentrations (Fig. 7B) was relatively low as compared with cells exposed to H_2O_2 (Fig. 7C,D). Ten minutes after H_2O_2 exposure, mitochondrial Ca^{2+} increased significantly and this was accompanied by MPT opening. Melatonin significantly reduced H_2O_2 stress-induced mitochondrial calcium rises (Fig. 7E,F) and cell blebbing. As the time course for mitochondrial calcium to increase was slightly after the rise in mitochondrial ROS, the H_2O_2-induced mitochondrial calcium increase probably

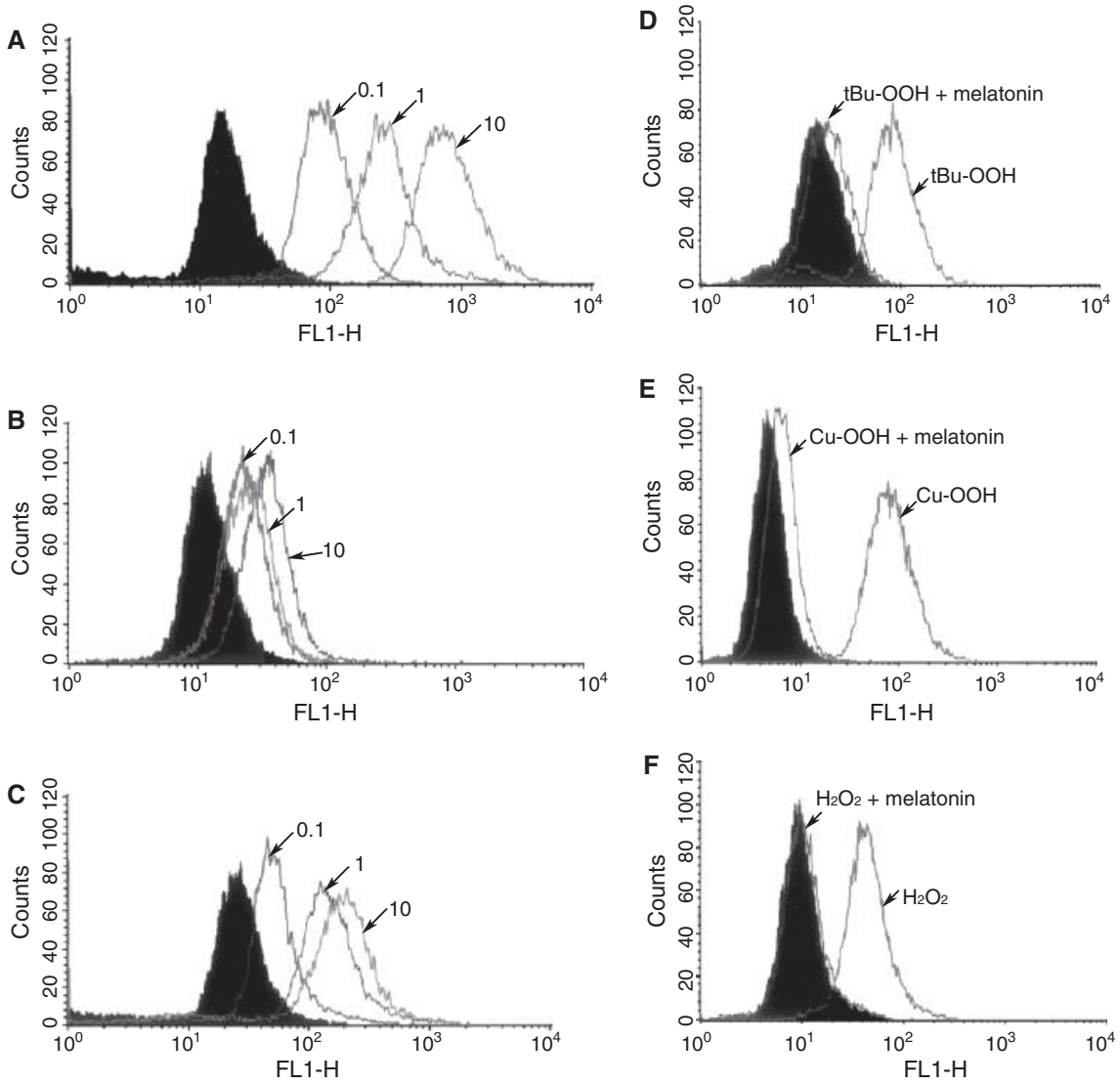

Fig. 5. Anti-oxidative effects provided by melatonin after stress caused by various oxidants and its comparison with vitamin E. (A) A dose-dependent increase in ROS formation induced by H_2O_2 (0.1, 1 and 10 mM); (B) 100 μM melatonin significantly reduced the H_2O_2 stress-induced ROS formation; (C) the anti-ROS effect of 100 μM vitamin E is less potent than that of melatonin during H_2O_2-induced-stress; (D, E) melatonin prevented mitochondrial ROS formation induced by short-chain oxidants *t*Bu-OOH and Cu-OOH, respectively, (F) ROS formation detected using D-123.

was secondary and was induced or enhanced by mitochondrial ROS formation.

Thereafter, we detected mitochondrial membrane potential changes using a mitochondrial membrane potential sensitive fluorescent probe, JC-1 (Fig. 8), and evaluated by laser scanning confocal microscopy. JC-1 measured both high (reported as j-aggregated red fluorescence) and low (reported as monomer green fluorescence) mitochondrial membrane potential. Confocal JC-1 images demonstrated that mitochondrial membrane potential in control RBA-1 cells was quite heterogeneous with both high (red fluorescence) and low (green fluorescence) mitochondrial membrane potentials being detected. The ratio of the populations of red to green mitochondria was about 2:3 (Fig. 8A,B). Soon after H_2O_2 exposure, mitochondrial membrane potential significantly depolarized, as shown by a dramatic shift of red fluorescence to green fluorescence (Fig. 8C,D). Also note that mitochondrial membrane potential depolarization was accompanied by the MPT opening. A quantity of 100 μM melatonin effectively prevented the mitochondrial membrane potential depolarization induced by H_2O_2 stress (Fig. 8E,F). The protection of mitochondrial membrane potential provided by melatonin was mainly due to its anti-mitochondrial ROS formation. Melatonin showed very little or no protective effect on mitochondrial membrane potential depolarization induced by either a high concentration of KCl (50 mM) or by a protonophore, (CCCP, 6 μM), which diminish mitochondrial proton gradients (data not shown).

Because mROS formation, membrane potential depolarization, mitochondrial swelling, as well as mitochondrial calcium overload have been shown to trigger the opening of the MPT and to release mitochondrial apoptotic lethal protein (cytochrome c) from mitochondrial membrane to

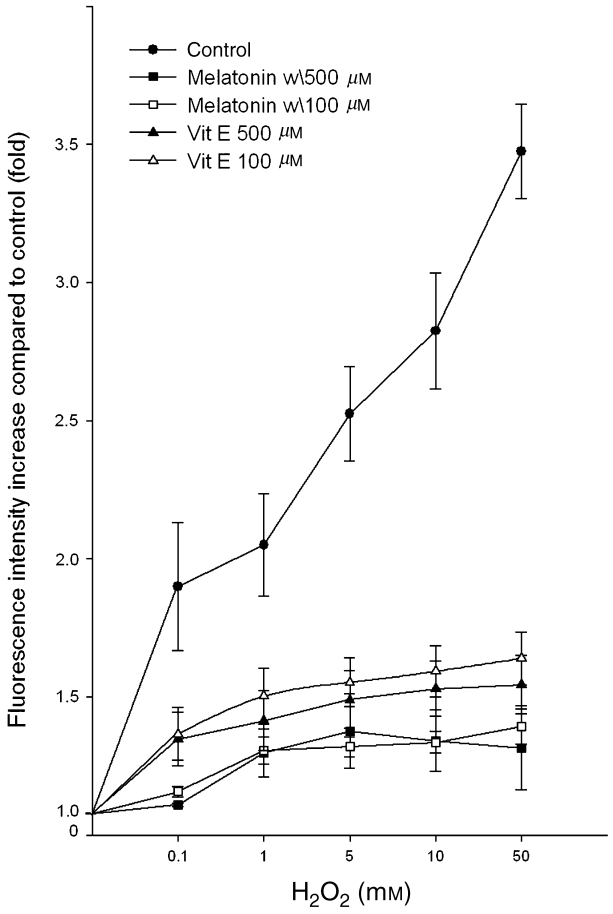

Fig. 6. A comparison of antioxidative effects provided by melatonin and vitamin E at different concentrations. After 30 min of melatonin and vitamin E treatment, ROS formation was detected by the fold increase in fluoresce intensity of ROS probe in cells exposed to H_2O_2 (0.1–50 mM). Antioxidative effects of 100 and 500 μM of melatonin and vitamin E were compared. Values are mean ± S.E.M. of five replicates from the same culture.

the cytosol, we examined whether melatonin would prevent H_2O_2 stress-induced cytochrome c release. The distribution of cytochrome c was detected using ICC and laser scanning confocal microscopy. The confocal images demonstrated that in a control cell cytochrome c was localized in the mitochondrial area (Fig. 9A). Another confocal image of a single cell taken at 90 min after the H_2O_2 exposure demonstrated cytochrome c release to the cytosolic and the nuclear area (Fig. 9B). Note that the release of cytochrome c coincided with shrinkage of the cell and mitochondrial swelling. The oxidant-induced cytochrome c release and cell shrinkage was dramatically prevented by melatonin (Fig. 9C). The cytochrome c-induced downstream activation of apoptotic enzyme, caspase 3, was also detected in the absence and the presence of melatonin in cells exposed to H_2O_2. The activity of caspase 3 was increased three- to fivefold at 150 min after the H_2O_2 stress. Melatonin, again, significantly prevented the activation of caspase 3 induced by the H_2O_2 stress in RBA-1 cells (data not shown).

To determine whether the anti-mitochondrial ROS effects provided by melatonin are critical for subsequent prevention of oxidant-induced apoptosis, we evaluated two early apoptotic events including the externalization of PS and YOPRO-1 staining of the early apoptotic nucleus. The flip-flop of PS from the inner to the outer plasma membrane leaflet during apoptosis is a common phenomenon of apoptosis occurring in many cell types independent of apoptotic inducers. Often, exposure of PS is reported to precede the opening of MPT, cell shrinkage, and nuclear condensation and can be independent of mitochondrial events including mitochondrial ROS formation, mitochondrial membrane potential depolarization and the release of cytochrome c. To simultaneously evaluate the precise time point of PS externalization and mitochondrial ROS formation during H_2O_2 stress, cells were co-incubated with Annexin V-FITC and D-123 for detecting the exposure of PS and mitochondrial ROS formation, respectively. Intriguingly, PS exposure appeared very quickly (within 10 min, Fig. 10B) after H_2O_2 exposure when mitochondrial ROS levels were only slightly elevated (Fig. 10A). These results indicate that low level of ROS formation may be sufficient for triggering PS externalization. We also investigated the specific time point for mitochondrial ROS formation in relation to the appearance of the early apoptotic nucleus. Cells were co-loaded with D-123 and YO-PRO-1 to simultaneously detect ROS formation and early nucleic acid staining respectively. In this case, the positive apoptotic nuclear staining appeared at a much later time point, i.e. 60 min post-H_2O_2 stress, and a positive YO-PRO-1 staining was detected concurrently with high mitochondrial ROS formation and mitochondrial swelling. Note that the morphology of nucleus at this time point was still normal in appearance (Fig. 10C). Melatonin effectively prevented both the PS externalization and positive YO-PRO-1 staining during H_2O_2 exposure (negative staining with Annexin V-FITC and YO-PRO-1, not shown).

Finally, we demonstrated that the potent anti-mitochondrial ROS induction of melatonin prevented the H_2O_2 stress-induced apoptosis. The H_2O_2-induced apoptotic cell death was evident by nuclear condensation, nuclear fragmentation (karyorrhexis) and DNA laddering. In Fig. 10D, superimposition of a DIC images with a fluorescent confocal PI images clearly demonstrate cell shrinkage, nuclear condensation as well as nuclear blebbing and karyorrhexis, typical markers of apoptosis, at 200 min after H_2O_2 stress (Fig. 10D). H_2O_2 stress-induced apoptosis was also apparent from the classic DNA laddering as detected by DNA gel electrophoresis. Again, melatonin effectively reduced H_2O_2 stress-induced apoptotic DNA laddering in RBA-1 cells (Fig. 10E).

Discussion

The advanced imaging tools employed in this study include time-lapse conventional, confocal, and multiphoton fluorescent imaging microscopy coupled with noninvasive mitochondria-targeted fluorescent probes. These tools provide a distinct opportunity for long-term visualization of the spatial and temporal dynamic profiles of mitochondrial function. The precise mechanism of action provided by melatonin at the mitochondrial level in live cells, therefore, can be studied exclusively throughout

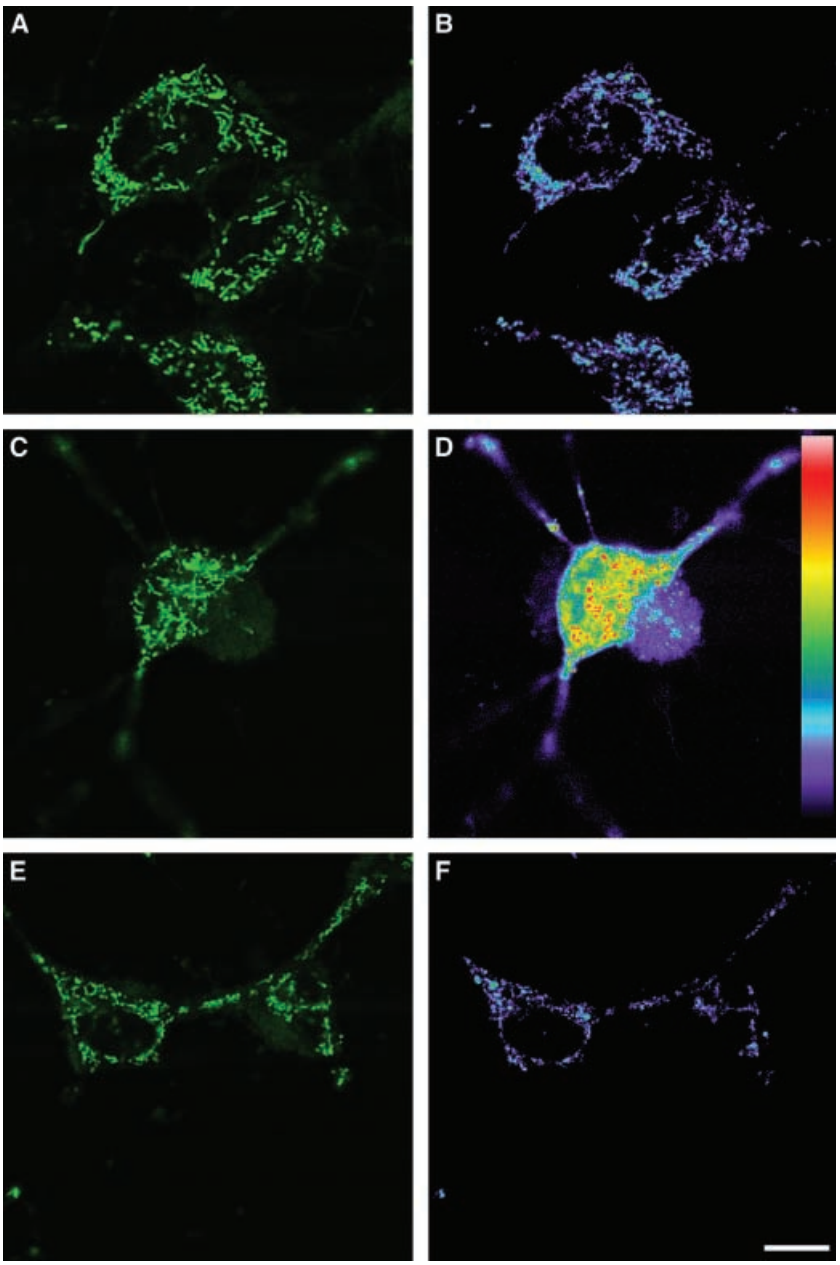

Fig. 7. Melatonin prevented mitochondrial calcium overload and MPT opening induced by H_2O_2 stress. Mitochondrial Ca^{2+} concentration and the MPT were concurrently imaged by dual labeling with a mitochondrial Ca^{2+} fluorescent probe, Rhod-2, and a mitochondrial fluorescent marker, Mito-G, by laser scanning confocal microscopy. (A, B) Control cells; (C, D) cells treated with the H_2O_2 without melatonin protection; (E, F) cells treated with the H_2O_2 with melatonin protection. (A, C, E) Mito-G images. (B, D, F) Mitochondrial Ca^{2+} images. Note mitochondria maintained in rod- or thread-like shape while mitochondrial Ca^{2+} was low. However, after H_2O_2 exposure, mitochondrial Ca^{2+} increased significantly and was accompanied by mitochondrial swelling as an indication of the MPT opening. Melatonin significantly prevented the H_2O_2 stress-induced mitochondrial Ca^{2+} increase and MPT opening. Bar, 10 μM.

H_2O_2 stress-induced apoptosis process. As a conclusion, we demonstrated for the first time that melatonin plays a pivotal role in protecting cells from H_2O_2 stress-induced apoptosis by targeting before 'the point of no return', the mitochondria. Mechanistic studies demonstrated that the indole significantly prevented mitochondrial dysfunction by reducing mitochondrial ROS formation during H_2O_2 stress. Via its ability to reduce mitochondrial ROS generation, melatonin prevented H_2O_2-induced mitochondrial calcium overload, mitochondrial membrane potential depolarization, and the opening of the MPT pore as demonstrated in this study. Subsequently, melatonin blocked MPT-dependent cytochrome c release, the downstream activation of caspase 3, the condensation of the nucleus and apoptotic fragmentation of nuclear DNA. Other early mitochondrial ROS-associated apoptotic events prevented by melatonin include the exposure of PS on the plasma membrane and the positive YOPRO-1 staining of early apoptotic nuclei.

In addition to its classical effects in the control of circadian rhythms and the regulation of the hypothalamo-pituitary-gonadal axis in seasonal breeding animals [41], the potent cytoprotective and anti-apoptotic effects provided by melatonin have recently secured extensive research attention [5, 9, 42–44]. The mechanisms of action for melatonin as a potent cytoprotector have been studied intensively. These actions include the ability of the indoleamine to act as a stimulator of the activities and mRNA levels of several antioxidant enzymes including SOD, GPx [5, 12], and GRx, as well as melatonin functioning as a stimulator of mitochondrial respiratory chain activity and ATP formation [12, 22, 27–29]. However, the

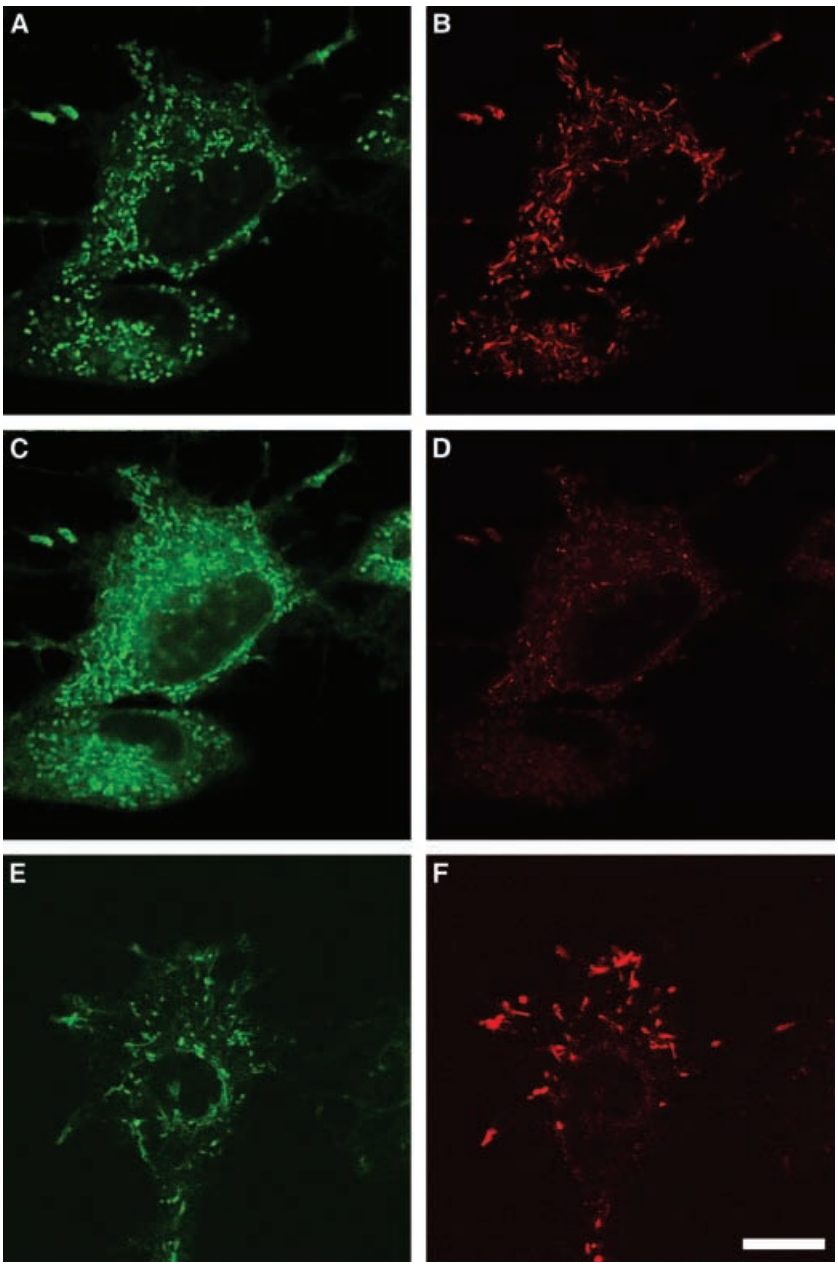

Fig. 8. Melatonin prevented mitochondrial membrane potential depolarization induced by H_2O_2. (A, B) Control; (C, D) cells treated with the H_2O_2 without melatonin protection; (E, F) cells treated with H_2O_2 with melatonin protection. Note the H_2O_2 stress caused a dramatic shift of the red fluorescence to green fluorescence due to mitochondrial membrane potential depolarization. 100 μM melatonin effectively prevented mitochondrial membrane potential depolarization induced by H_2O_2 stress. Bar, 10 μM.

functional expression of genes for antioxidative enzymes may require hours to days and, therefore, may not be sufficient for antagonizing instantaneously formed ROS during oxidative stress. Rapid mitochondrial ROS formation has been demonstrated in this study as well as in our previous observations [30, 36, 45]. Substantial increases in mitochondrial ROS formation appeared almost immediately after cells were exposed to H_2O_2 stress or photoirradiation. To effectively counteract the rapidly formed mitochondrial ROS, melatonin must act as a potent ROS scavenger. The highly lipophilic property of the indole molecule readily allows melatonin to pass through the plasma membrane and enter the mitochondrial compartment [46, 47] where it exerts potent antioxidative effects. In this study, we found that as long as melatonin was administered before the induction of H_2O_2-induced mitochondrial ROS formation, it significantly reduced the damage to the mitochondria and prevented the subsequent H_2O_2-induced apoptosis. This suggests that the anti-mitochondrial ROS formation effect of melatonin is a primary and key mechanism in averting mitochondrial dysfunction and cell damage induced by H_2O_2. The astonishingly rapid and effective anti-mitochondrial ROS formation provided by melatonin may arise from the fact that melatonin is an electron-rich molecule. Melatonin can donate two electrons in the redox reactions which makes it a potent antioxidant and free radical scavenger and it effectively scavenges $^1O_2$, H_2O_2 and the devastatingly toxic $^{\bullet}OH$, [10, 13, 48]. In addition, the metabolites of melatonin are also potent antioxidants; these include N^1-acetyl-N^2-formyl-5-methoxy kynuramine and *N*-acetyl-5-methoxykynuramine [10, 11, 48]. By scavenging the highly toxic

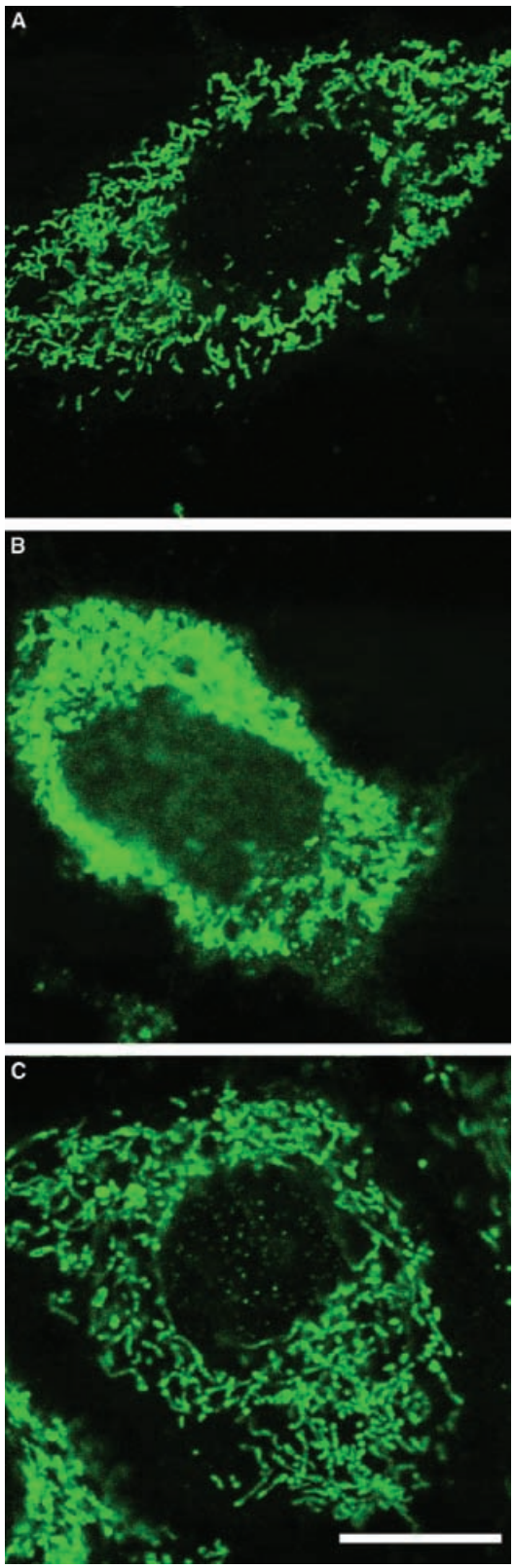

Fig. 9. Melatonin prevented cytochrome c release induced by H_2O_2. (A) Control; (B) cell treated with H_2O_2; (C) melatonin protected cell treated with H_2O_2. Cytochrome c was detected by an immunocytochemistry method using confocal microscopy. Bar, 10 μM.

•OH, melatonin counteracts lipid peroxidation and averts the oxygen radical attack to cytosolic proteins and DNA [3, 49].

In addition to H_2O_2-induced damage, our data also demonstrate that melatonin prevent mitochondrial ROS formation induced by other short-chain organic hydroperoxides including *t*Bu-OOH and Cu-OOH. These short-chain organic hydroperoxides induce mitochondrial damage similar to that seen in pathological mitochondrial ROS induced oxidative damage in various diseases [50]. Recently, it was reported that mitochondria contain nitric oxide synthase (NOS) which may be responsible for the subsequent formation of reactive nitrogen species (RNS), e.g. peroxynitrite anion ($ONOO^-$), and the RNS-induced cellular damage [51, 52]. Melatonin has been reported also to inhibit NOS or to directly scavenge NO, $ONOO^-$ and peroxynitrous acid [9, 11, 13]. Therefore, melatonin may also protect cells by reducing mitochondrial RNS formation. Collectively, these findings together may explain why melatonin is superior to other antioxidants such as vitamin C, vitamin E, *N*-acetlycysteine, and glutathione as seen in this study and by others [6, 8, 30, 50, 53].

Mitochondria are not only a major site of ROS generation but also the main target of ROS. Thus, it is important to protect mitochondria from being damaged during oxidative stress. Based on studies in liver and kidney preparations, it was concluded that it is the depletion of mitochondrial antioxidants such as GSH rather than reduction of the cytosolic antioxidant pool which is critical for development of irreversible cellular damage [54]. Mitochondrial ROS levels in resting cells are higher than ROS levels in other compartments. As demonstrated in this study, the level of ROS in the nucleus or the cytosol area was one-third of that in mitochondria. High levels of resting mitochondrial ROS are attributed to the fact that up to 4% of the oxygen consumed by the mitochondrial respiratory chain undergoes one electron reduction via the semiquinone form of coenzyme Q to generate the superoxide radicals and, via the complexes I and III of mitochondrial ETC, to generate other ROSs. Unavoidably, these newly formed ROS target the mitochondria themselves and induced even more ROS formation. Mitochondrial dysfunctions induced by ROS include disruption of membrane structure and the integrity of ETC, a diminished proton gradient and intra-mitochondrial redox status, and finally cessation of ATP generation. Further, as shown by current study and by our previous work, stress induced by mitochondrial ROS formation or neurotransmitters can cause severe mitochondrial calcium dysregulation which results in mitochondrial calcium overload [31, 45, 55]. Synergistically, high levels of ROS and mitochondrial calcium overload triggers the opening of the MPT to release mitochondrial lethal proteins such as cytochrome c, which was also documented in this study. Furthermore, we demonstrated that the activated caspase 3 induced by H_2O_2 stress caused cells to undergo nuclear chromatin condensation and DNA fragmentation, typical characters apoptotic cell death. Thus, the potent action of melatonin at the proper spatial and temporal point to prevent mitochondrial ROS formation may explain how the indole molecule can effectively

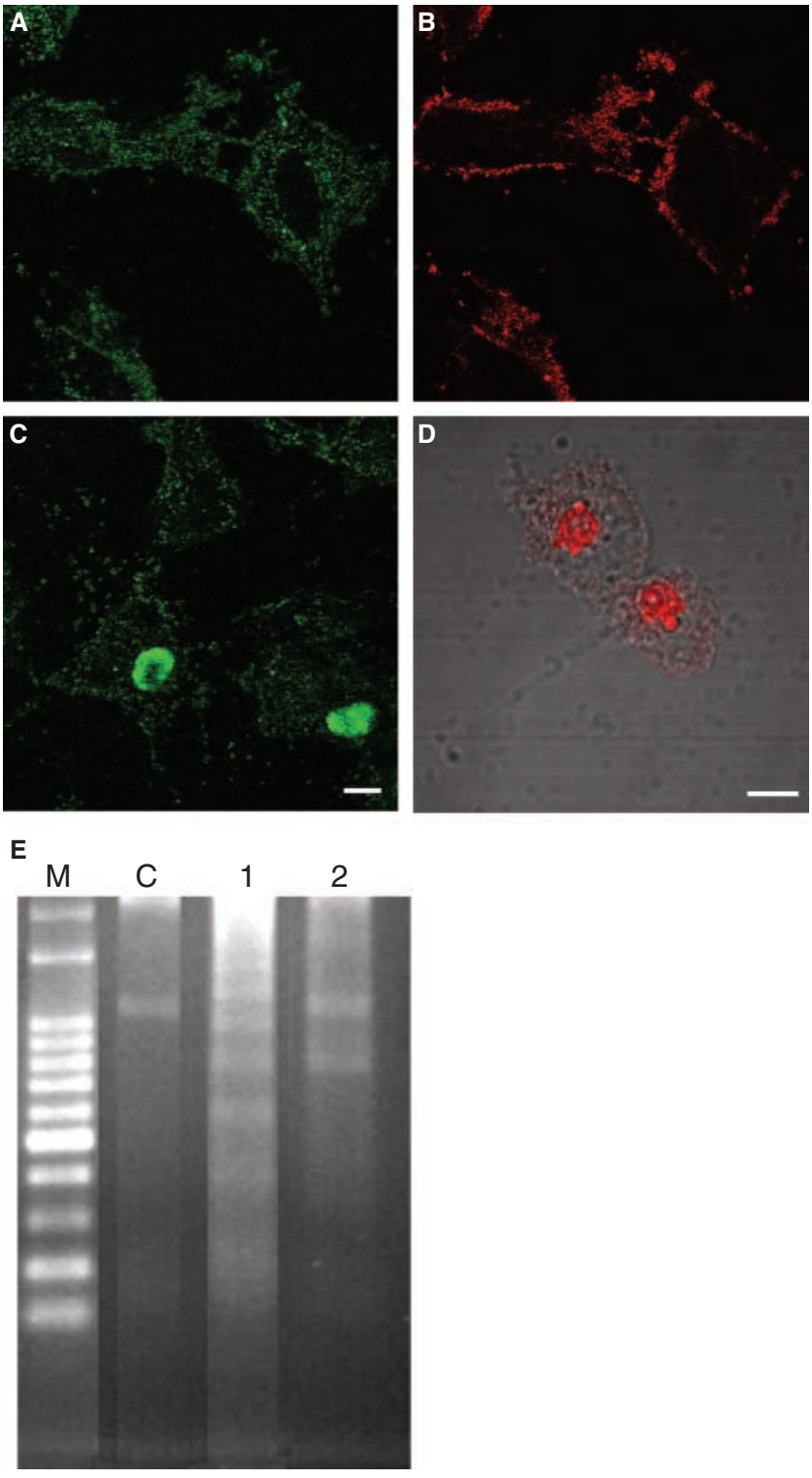

Fig. 10. Rises in mitochondrial ROS caused early and late apoptotic events and were prevented by melatonin. (A–C) Early apoptotic events: simultaneous detection of mitochondrial ROS level (A) and the externalization of PS (B) using D-123 and Annexin-V, respectively, at 5 min after initiation of oxidative stress; (C) simultaneous detection of mitochondrial ROS formation and early apoptotic nuclei using D-123 and YOPRO-1 staining, respectively, at 60 min after initiation of oxidative stress. (D) Late apoptotic events including condensation and karyorrhexis (blebbing and fragmentation) of the nuclei at 200 min after H_2O_2 stress. All of the mitochondrial ROS-dependent events including the PS exposure, the YOPRO-1 staining of early apoptotic nuclei and the condensation and karyorrhexis (blebbing and fragmentation) of the nuclei were prevented by melatonin (data not shown). (E) DNA laddering gel. M, makers; C, control; 1, cells treated with H_2O_2; 2, melatonin protected cells treated with H_2O_2. Bar, 10 μM.

reduce cell damage and death from various oxidative stresses or toxins including 6-hydroxydopamine, [24, 25, 56], 1-methyl-4-phenylpyridinium [26], ruthenium red [50], and kainate [24, 57]. The protective actions at the mitochondrial level are summarized in Fig. 11. Of interest is the fact that melatonin concentrations with in the mitochondria of cells are reportedly higher than these in the systemic circulation [17]. This is likely consistent with an action of the indoleamine at the mitochondrial level. Additionally the current results which document a great protective effect of melatonin, over that of vitamin E, in the mitochondria is also in line with observations of Martin et al [17]. This latter group, as with the current findings, show that melatonin was more effective than vitamin E or C in limiting the toxicity of *t*Bu-OOH at the mitochondrial level.

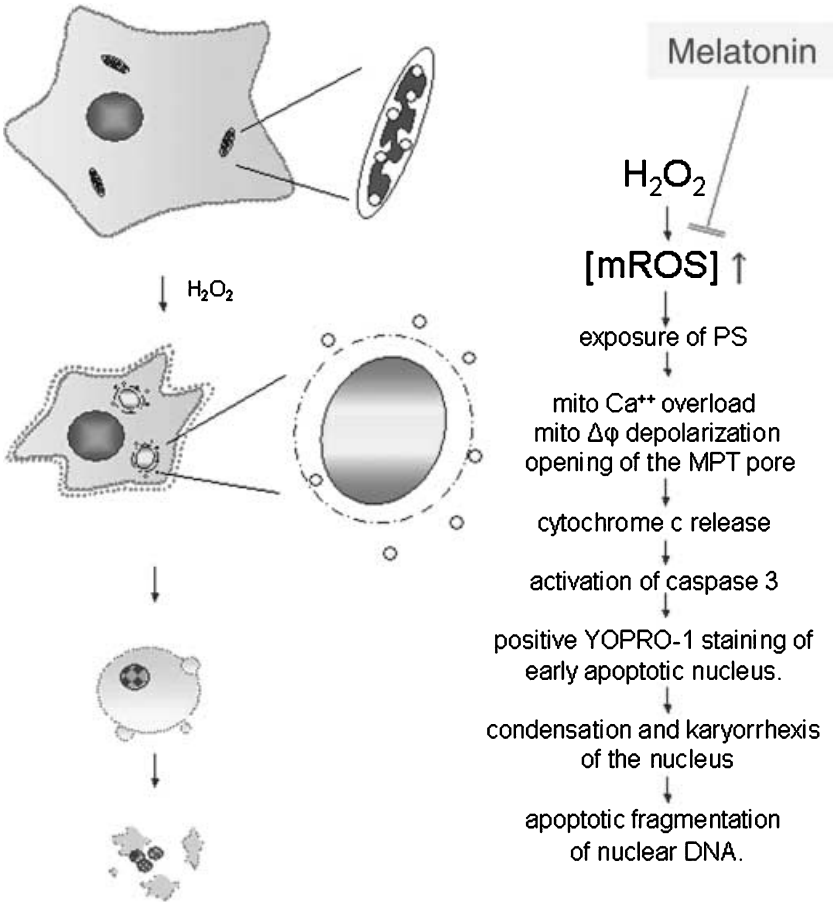

Fig. 11. Schematic diagram of the mechanisms of action of melatonin at the mitochondrial level in limiting oxidative stress-induced apoptosis. The indole significantly reduces mitochondrial ROS formation induced by H_2O_2. Via its potent inhibitory effect on mitochondrial ROS generation, melatonin prevents the externalization of PS, mitochondrial calcium overload, mitochondrial membrane potential depolarization, and the opening of the MPT. Subsequently, melatonin blocks MPT-dependent cytochrome c release, downstream activation of caspase 3, and the condensation and karyorrhexis of the nuclei and apoptotic fragmentation of nuclear DNA.

Prevention of ROS-induced glial cell dysfunction is of significance as accumulating evidence implies that glial cells play a critical role in maintaining the integrity of the central nervous system. Glial cells can protect neurons from various stress-induced neurotoxicities [58]. Glial cells also enhance neuronal survival during pathological conditions such as sepsis and age-related neurodegeneration including Parkinson's disease and Alzheimer's disease [1, 56]. More recently, ROS-induced inflammatory responses of glial cells have been reported to be closely associated with the activity of neural stem cells in the hippocampus [59]. In addition to classical treatment with nonsteroidal anti-inflammatory drugs, consumption of melatonin as a regular antioxidant vitamin [6] may provide an effective way of restoring neurogenesis and neuroplasticity in patients suffering with ROS neuronal stress. Additional clinical application of melatonin proposed include its immunomodulatory effect for protection against [60], radiation-induced and chemotherapeutic drug-induced toxicity [42] effects on cell growth, metabolic activity and cell cycle distribution [61], delta-aminolevulinic acid-induced cancer [62] and correction on senescence-induced mitochondrial dysfunction [29]. Thus, the powerful protection provided by melatonin at the mitochondrial level re-emphasizes its therapeutic potential to combat a variety of oxidative stress-induced mitochondrial dysfunctions as well as mitochondria-mediated apoptosis in various diseases [63].

Acknowledgments

This research work was supported by grants CMRP 1009 (to M-JJ) and CMRP 930 (to T-IP) from the Chang Gung Medical Research Foundation, grants NSC 89-2320-B-182-089 and NSC 90-2315-B-182-006 (to M-JJ), and NSC 91-2314-B-182A-021 (to T-IP) from the National Science Council, Taiwan, and grant DMR-91-009 (to S-BJ) from China Medical College, Taiwan.

Supplementary Material

An interactive online version of the active process detailed in Fig. 2 is documented in a time-lapse movie file which can be found at the following web address: http://163.25.114.8/mei-jie/_private/melatonin_jpr_2004.htm

References

1. Coyle JT, Puttfarcken P. Oxidative stress, glutamate, and neurodegenerative disorders. Science 1993; **262**:689–695.
2. Beal MF. Mitochondrial dysfunction in neurodegenerative diseases. Biochim Biophys Acta 1988; **1366**:211–223.
3. Reiter RJ, Guerrero JM, Garcia JJ, Acuna-Castroviejo D. Reactive oxygen intermediates, molecular damage, and aging: relation to melatonin. Ann N Y Acad Sci 1998; **854**:410–424.

4. Halliwell B, Gutteridge JMC. Free Radicals in Biology and Medicine, 3rd edn. Oxford University Press, Oxford, 1999.
5. Reiter RJ, Tan DX, Osuna C, Gitto E. Actions of melatonin in the reduction of oxidative stress: a review. J Biomed Sci 2000; **7**:444–458.
6. Tan DX, Manchester LC, Hardeland R et al. Melatonin: a hormone, a tissue factor, an autocoid, a paracoid, and an antioxidant vitamin. J Pineal Res 2003; **34**:75–78.
7. Tan DX, Chen LD, Poeggeler B, Manchester LC, Reiter RJ. Melatonin: a potent, endogenous hydroxyl radical scavenger. Endocrine J 1993; **1**:57–60.
8. Pieri C, Marra M, Moroni F, Recchioni R, Marcheselli F. Melatonin: a peroxyl radical scavenger more effective than vitamin E. Life Sci 1994; **55**:L271–L276.
9. Reiter RJ, Tan DX, Manchester LC, Qi W. Biochemical reactivity of melatonin with reactive oxygen and nitrogen species: a review of the evidence. Cell Biochem Biophys 2001; **34**:237–256.
10. Tan DX, Manchester LC, Reiter RJ et al. Melatonin directly scavenges hydrogen peroxide: a potentially new metabolic pathway of melatonin biotransformation. Free Radic Biol Med 2000; **29**:1177–1185.
11. Allegra M, Reiter RJ, Tan DX, Gentile C, Tesoriere L, Livrea MA. The chemistry of melatonin's interaction with reactive species. J Pineal Res 2003; **34**:1–10.
12. Rodriguez C, Mayo JC, Sainz RM et al. Regulation of antioxidant enzymes: a significant role for melatonin. J Pineal Res 2004; **36**:1–9.
13. Tan DX, Manchester LC, Reiter RJ, Qi WB, Karbownik M, Calvo JR. Significance of melatonin in antioxidative defense system: reactions and products. Biol Signals Recept 1993; **9**:137–159.
14. Melchiorri D, Reiter RJ, Sewerynek E, Chen LD, Nistico G. Melatonin reduces kainate-induced lipid peroxidation in homogenates of different brain regions. FASEB J 1995; **9**:1205–1210.
15. Antolin I, Rodriguez C, Sainz RM et al. Neurohormone melatonin prevents cell damage: effect on gene expression for antioxidant enzymes. FASEB J 1996; **10**:882–890.
16. Okatani Y, Wakatsuki A, Kaneda C. Melatonin increases activities of glutathione peroxidase and superoxide dismutase in fetal rat brain. J Pineal Res 2000; **28**:89–96.
17. Martin M, Macias M, Escames G, Leon J, Acuña-Castroviejo D. Melatonin but not vitamins C and E maintains glutathione homeostasis in t-butyl hydroperoxide-induced mitochondrial oxidative stress. FASEB J 2000; **14**:1677–1679.
18. Reiter RJ, Tan DX, Burkhardt S. Reactive oxygen and nitrogen species and cellular and organismal decline: amelioration with melatonin. Mech Ageing Dev 2002; **123**:1007–1019.
19. Lopez-Burillo S, Tan DX, Rodriquez-Gallego V et al. Melatonin and its derivatives cyclic 3-hydroxymelatonin, N^1-methyl-N^2-formyl-5-methoxytryptamine and 6-hydroxymelatonin reduce oxidative DNA damage included by Fenton reagents. J Pineal Res 2003; **34**:178–184.
20. Sener G, Sehirli AO, Paskaloglu K, Dülger GA, Alican I. Melatonin treatment protects against ischemia/reperfusion-induced functional and biochemical changes is rat urinary bladder. J Pineal Res 2003; **34**:226–230.
21. Acuña-Castroviejo D, Martin M, Macias M et al. Melatonin, mitochondria, and cellular bioenergetics. J Pineal Res 2001; **30**:65–74.
22. Okatani Y, Wakatsuki A, Reiter RJ. Melatonin and mitochondrial respiration. In: Melatonin: Biological Basis of its Function in Health and Disease, Chapter 2, pp 11–24. Pandi-Perumal SR, Cardinali DP eds., Londes Bioscience, Georgetown, 2004.
23. Yamamoto H, Tang HW. Preventive effect of melatonin against cyanide-induced seizures and lipid peroxidation in mice. Neurosci Lett 1996; **207**:89–92.
24. Dabbeni S, Floreani M, Franceschini D, Skaper SD, Giusti P. Kainic acid induces selective mitochondrial oxidative phosphorylation enzyme dysfunction in cerebellar granule neurons: protective effects of melatonin and GSH ethyl ester. FASEB J 2001; **15**:1786–1788.
25. Dabbeni-Sala F, Di Santo S, Franceschini D, Skaper SD, Giusti P. Melatonin protects against 6-OHDA-induced neurotoxicity in rats: a role for mitochondrial complex I activity. FASEB J 2001; **15**:164–170.
26. Absi E, Ayala A, Machado A, Parrado J. Protective effect of melatonin against the 1-methyl-4-phenylpyridinium-induced inhibition of complex I of the mitochondrial respiratory chain. J Pineal Res 2000; **29**:40–47.
27. Martin M, Macias M, Leon J, Escames G, Khaldy H, Acuna C. Melatonin increases the activity of the oxidative phosphorylation enzymes and the production of ATP in rat brain and liver mitochondria. Int J Biochem Cell Biol 2002; **34**:348–357.
28. Okatani Y, Wakatsuki A, Reiter RJ, Miyahara Y. Acutely administered melatonin restores hepatic mitochondrial physiology in old mice. Int J Biochem Cell Biol 2003; **35**:367–375.
29. Okatani Y, Wakatsuki A, Reiter RJ, Enzan H, Miyahara Y. Protective effect of melatonin against mitochondrial injury induced by ischemia and reperfusion of rat liver. Eur J Pharmacol 2003; **469**:145–152.
30. Jou MJ, Jou SB, Chen HM, Lin CH, Peng TI. Critical role of mitochondrial reactive oxygen species formation in visible laser irradiation-induced apoptosis in rat brain astrocytes (RBA-1). J Biomed Sci 2002; **9**:507–516.
31. Peng TI, Wei YH, Wu HY, Jou MJ. Mitochondrial calcium and ROS mediated apoptosis plays a potential pathogenic role in diseases associated with mitochondrial DNA 4977bp deletion. Biophys J 2003; **84**:205a.
32. Sohal RS, Brunk UT. Mitochondrial production of pro-oxidants and cellular senescence. Mutat Res 1992; **275**:295–304.
33. Skulachev VP. Mitochondrial physiology and pathology; concepts of programmed death of organelles, cells and organisms. Mol Aspects Med 1999; **20**:139–184.
34. Nicholls DG, Budd SL. Mitochondria and neuronal survival. Physiol Rev 2000; **80**:315–360.
35. Jou TC, Jou MJ, Chen YY, Lee SY. Properties of rat brain astrocytes in long-term culture (in Chinese). J Formosan Med Assoc 1985; **84**:865–881.
36. Peng TI, Jou MJ. Photo-irradiation induced heterogenous intracellular reactive oxygen species formation and mitochondrial permeability transition pore opening revealed by multiphoton imaging microscopy. Ann N Y Acad Sci 2004; **1011**:11–23.
37. LeBel CP, Ischiropoulos H, Bondy SC. Evaluation of the probe 2′, 7′-dichlorofluorescin as an indicator of reactive oxygen species formation and oxidative stress. Chem Res Toxicol 1992; **5**:227–231.
38. Idziorek T, Estaquier J, De B, Ameisen JC. YOPRO-1 permits cytofluorometric analysis of programmed cell death (apoptosis) without interfering with cell viability. J Immunol Methods 1995; **185**:249–258.

39. Martin SJ, Reutelingsperger CP, McGahon AJ et al. Early redistribution of plasma membrane phosphatidylserine is a general feature of apoptosis regardless of the initiating stimulus: inhibition by overexpression of Bcl-2 and Abl. J Exp Med 1995; **182**:1545–1556.
40. Denecker G, Dooms H, Van Loo G et al. Phosphatidyl serine exposure during apoptosis precedes release of cytochrome c and decrease in mitochondrial transmembrane potential. FEBS Lett 2000; **465**:47–52.
41. Reiter RJ. The pineal and its hormones in the control of reproduction in mammals. Endocr Rev 1980; **1**:109–131.
42. Reiter RJ, Tan DX, Sainz RM, Mayo JC, Lopez-Burillo S. Melatonin: reducing the toxicity and increasing the efficacy of drugs. J Pharm Pharmacol 2002; **54**:1299–1321.
43. Hardeland R, Poeggeler B, Niebergall R, Zelosko V. Oxidation of melatonin by carbonate radicals and chemiluminescence emitted during pyrrole ring cleavage. J Pineal Res 2003; **34**:17–25.
44. Tan DX, Hardeland R, Manchester LC et al. Mechanistic and comparative studies of melatonin and classic antioxidants in terms of their interactions with the ABTS cation radical. J Pineal Res 2003; **34**:249–259.
45. Jou MJ, Jou SB, Guo MJ, Wu HY, Peng TI. Mitochondrial reactive oxygen species generation and mitochondrial calcium increase induced by visible light in astrocytes. Ann N Y Acad Sci; **1011**:45–56.
46. Menendez-Pelaez A, Reiter RJ. Distribution of melatonin in mammalian tissues: the relative importance of nuclear versus cytosolic localization. J Pineal Res 1993; **15**:59–69.
47. Poon AM, Pang SF. 2[125I]iodomelatonin binding sites in spleens of guinea pigs. Life Sci 1992; **50**:1719–1726.
48. Tan DX, Manchester LC, Burkhardt S et al. N^1-acetyl-N^2-formyl-5-methoxykynuramine, a biogenic amine and melatonin metabolite, functions as a potent antioxidant. FASEB J 2001; **15**:2294–2296.
49. Reiter RJ, Melchiorri D, Sewerynek E et al. A review of the evidence supporting melatonin's role as an antioxidant. J Pineal Res 1995; **18**:1–11.
50. Martin M, Macias M, Escames G et al. Melatonin-induced increased activity of the respiratory chain complexes I and IV can prevent mitochondrial damage induced by ruthenium red in vivo. J Pineal Res 2000; **28**:242–248.
51. Ghafourifar P, Richter C. Nitric oxide synthase activity in mitochondria. FEBS Lett 1997; **418**:291–296.
52. Giulivi C. Characterization and function of mitochondrial nitric-oxide synthase. Free Radic Biol Med 2003; **34**:397–408.
53. Khaldy H, Escames G, Leon J, Vives F, Luna JD, Acuña-Castroviejo D. Comparative effects of melatonin, L-deprenyl, Trolox and ascorbate in the suppression of hydroxyl radical formation during dopamine autoxidation in vitro. J Pineal Res 2000; **29**:100–107.
54. Miccadei S, Kyle ME, Gilfor D, Farber JL. Toxic consequence of the abrupt depletion of glutathione in cultured rat hepatocytes. Arch Biochem Biophys 1988; **265**:311–320.
55. Wang H, Joseph JA. Mechanisms of hydrogen peroxide-induced calcium dysregulation in PC12 cells. Free Radic Biol Med 2000; **28**:1222–1231.
56. Mayo JC, Sainz RM, Uria H, Antolin I, Esteban MM, Rodriguez C. Melatonin prevents apoptosis induced by 6-hydroxydopamine in neuronal cells: implications for Parkinson's disease. J Pineal Res 1998; **24**:179–192.
57. Giusti P, Lipartiti M, Franceschini D, Schiavo N, Floreani M, Manev H. Neuroprotection by melatonin from kainate-induced excitotoxicity in rats. FASEB J 1996; **10**:891–896.
58. Bronstein DM, Perez O, Sun V et al. Glia-dependent neurotoxicity and neuroprotection in mesencephalic cultures. Brain Res 1995; **704**:112–116.
59. Kempermann G, Neumann H. Microglia: the enemy within? Science 2003; **302**:1689–1690.
60. Vijayalaxmi, Thomas CR, Reiter RJ, Herman TS. Melatonin: from basic research to cancer treatment clinics. J Clin Oncol 2002; **20**:2575–2601.
61. Natarajan M, Reiter RJ, Meltz ML, Herman TS. Effect of melatonin on cell growth, metabolic activity, and cell cycle distribution. J Pineal Res 2001; **31**:228–233.
62. Karbownik M, Reiter RJ. Melatonin protects against oxidative stress caused by delta-aminolevulinic acid: implications for cancer reduction. Cancer Invest 2002; **20**:276–286.
63. Acuña-Castroviejo D, Escames G, Carozo A, Leon J, Khaldy H, Reiter RJ. Melatonin, mitochondrial homeostasis and mitochondrial-related diseases. Curr Top Med Chem 2002; **2**:133–152.